Numerical Study of the Rainfall Event due to the Interaction of Typhoon Babs (1998) and the Northeasterly Monsoon

Chun-Chieh Wu

Department of Atmospheric Sciences, National Taiwan University, Taipei, Taiwan

Kevin K. W. Cheung

Climate Risk Concentration of Research Excellence, and Department of Environment and Geography, Macquarie University, Sydney, Australia

Ya-Yin Lo

Department of Atmospheric Sciences, National Taiwan University, Taipei, Taiwan

ABSTRACT

A heavy rainfall event in the Taiwan area associated with the interaction between Typhoon Babs (1998) and the East Asia winter monsoon is studied. Typhoon Babs is a case in point demonstrating the often-observed phenomenon that heavy rainfall can be induced in the eastern and/or northeastern region of Taiwan. Such heavy rainfall was caused by the joint convergent flow associated with the outer circulation of typhoons and the strengthening northeasterly monsoon in late typhoon season, even though Babs remained distant from Taiwan when it moved through the island of Luzon in the Philippines and stayed over the South China Sea. This heavy rainfall event is simulated in this study using the fifth-generation Pennsylvania State University–National Center for Atmospheric Research (PSU–NCAR) Mesoscale Model (MM5) with three nested domains and a highest horizontal resolution of 6.67 km. The control experiments with Kain–Fritsch cumulus parameterization perform well in terms of both simulated track and intensity. The 20-km resolution simulation reproduces the correct rainfall distribution during the three days studied, and the fine domain with 6.67-km resolution further improves the maximum simulated rainfall to very close to the observations. A series of sensitivity experiments that include model physics, terrain effect, typhoon vortex structure, and monsoon strength is performed, aiming at investigating the predictability of this typhoon–monsoon–terrain system when some of its components are perturbed. The rainfall event is analyzed based on two rainfall modes of different dominant mechanisms: monsoon mode during 0000 UTC 24–25 October and topographic mode during 0000 UTC 25–26 October. Removal of the Taiwan terrain in one of the sensitivity experiments results in completely different rainfall distribution due to the lack of the convection by orographic lifting, and the terrain is also found to play a key role in changing the low-level convergence pattern between the typhoon circulation and monsoonal northeasterlies. When the radius of the bogus vortex is reduced, the cold front to the north migrates southward in a faster pace than in the control simulation, and rain rate at the front also increases such that total accumulated rainfall at northern Taiwan is comparable with that in the control simulation but with shifted maximum position. In the extreme case in which no bogus vortex is implanted at all, rainfall is mainly associated with evolution of the cold front (pure frontal mode). In addition, a technique is developed to modify the monsoon strength over China. It is found that low-level (1000–700 hPa) reduction in monsoon strength weakens interaction with the typhoon, and rain distribution remains the same as in the control simulation. However, the simulated typhoon track is considerably sensitive to the deep-layer (1000–300 hPa) monsoon strength.

1. Introduction

The direct threats a tropical cyclone (TC) poses to human lives and properties mainly come from its destructive winds and heavy rainfall, which are of concern to all coastal areas in Southeast Asia. Taiwan is usually

Corresponding author address: Chun-Chieh Wu, Dept. of Atmospheric Sciences, National Taiwan University, 1, Sec. 4, Roosevelt Rd., Taipei 106, Taiwan.
E-mail: cwu@typhoon.as.ntu.edu.tw

impacted by an average of about three to four TCs every year. Some of these TCs affecting Taiwan form in the monsoon trough east of the Philippines, while the others form in the South China Sea (SCS). Those TCs traveling westward in the western North Pacific (WNP) usually make landfall along the east coast of Taiwan, while those originating in the SCS usually land at the southern/southwestern side. Given the different landfall positions, the rainfall distribution over Taiwan is quite different (Cheung et al. 2008). In addition to the destruction brought about by strong winds, the continuous heavy rainfall causes flooding, landslides, and debris flows.

In general, TC-related rainfall distribution depends much on the internal structure of the TC. For example, the size of the eyewall determines to first order the location of the maximum rain rate (Lonfat et al. 2004). Asymmetry in the eyewall convection and mesoscale convective systems embedded in the TC are also important factors. For Taiwan, two other factors influence the local TC-related rainfall to a large extent and cause much forecast difficulty: (i) the topographical effect of the Central Mountain Range (CMR); and (ii) interaction of the approaching TC with the Asian monsoon system. Because the CMR has an average height of about 3 km, it can deflect the motion of an approaching TC, and modify the structure and rainfall distribution. Therefore, the terrain-interaction problem has led to a number of studies (e.g., Brand and Blelloch 1974; Bender et al. 1987; Chang 1982; Yeh and Elsberry 1993a,b; Chang et al. 1993; Wu and Kuo 1999; Wu 2001; Wu et al. 2002; Lin et al. 2002; Chiao and Lin 2003; Lin et al. 2005; Jian and Wu 2008). By comparison, few systematic studies have been done on the interaction with the monsoon system. When a TC is near the boundary between the WNP and SCS in the summer, the low pressure associated with the TC seems to enhance the monsoonal southwesterly, and the stronger southwesterly interacting with the Taiwan topography influences the rainfall distribution associated with the TC. A well-known example of this kind of scenario occurred in Typhoon Mindulle (2004) with torrential rainfall over southwestern Taiwan (Chien et al. 2008; Lee et al. 2008).

During autumn or early winter, the warm, moist air in TC circulation can interact with the cold, dry winter-monsoonal northeasterlies and create a frontal-type system that brings even more rainfall to certain regions in Taiwan. In some of these cases, the TC did not make landfall in Taiwan, and its center is quite far away from the island. A classic case with this scenario is Supertyphoon Lynn (1987) that formed near the island of Pohnpei (~6.9°N, 158.2°E) in mid-October and later reached its peak intensity of 140 kt (72 m s^{-1}) during 0000 UTC 20 October–0000 UTC 21 October when it

moved westward and northwestward. When Lynn entered the Luzon Strait at 0000 UTC 24 October and later made landfall near Hong Kong, the typhoon was in its weakening phase (see location of places in Fig. 2a). However, Taiwan still experienced torrential rainfall and high winds when Lynn's center was over 200 km from southwestern Taiwan (and over 400 km from its northern region). The Central Weather Bureau (CWB) of Taiwan recorded 1730 mm of rainfall in the Taipei area and 1915 mm at Yangming Mountain in northern Taiwan. In addition, sustained surface wind speed of 84 kt (43 m s^{-1}) was recorded in Taipei at 0000 UTC 24 October while the typhoon intensity reached 90 kt (ATCR 1987), indicating that the high wind speed was the result of combined effect with the monsoonal flow. Over 2000 people were affected by floods, and about 60 residents were reported perished or missing.

Because the temporal and spatial rainfall patterns under the interaction of TC circulation and the monsoon system deviate substantially from usual TC rainfall climatology, being able to predict the rainfall pattern based on numerical models is important. Therefore, a more recent case of Typhoon Babs in 1998 is studied using a numerical weather prediction model. The synoptic background of Babs and distribution of associated rainfall are first described in section 2. The numerical model and configuration used are described in section 3. In section 4, results from the control experiment and a series of sensitivity experiments for identifying the dynamical factors that affect the rainfall and wind distribution are described. The predictability of this rainfall event based on system interaction as revealed by these sensitivity experiments is also discussed. Finally, summary and concluding discussions are provided in section 5.

2. Synoptic environment associated with Typhoon Babs

Typhoon Babs developed from a tropical disturbance southwest of Guam and reached tropical storm intensity at 0006 UTC 15 October 1998 (ATCR 1998) when it moved westward toward the Philippines. Interaction with a tropical upper tropospheric trough (TUTT) caused the cyclone to slow down because the subtropical ridge was weakened. After the TUTT's negative influence to the cyclone's upper-level outflow ended, Babs intensified to supertyphoon (maximum intensity ~135 kt) just before making landfall in the Philippines. Then the cyclone weakened slightly after passing through central Luzon at around 0000 UTC 23 October because of interaction with land. When Babs was in the SCS, it approached the monsoonal cold high in mainland China and frontal systems. Starting 0000 UTC 25 October the
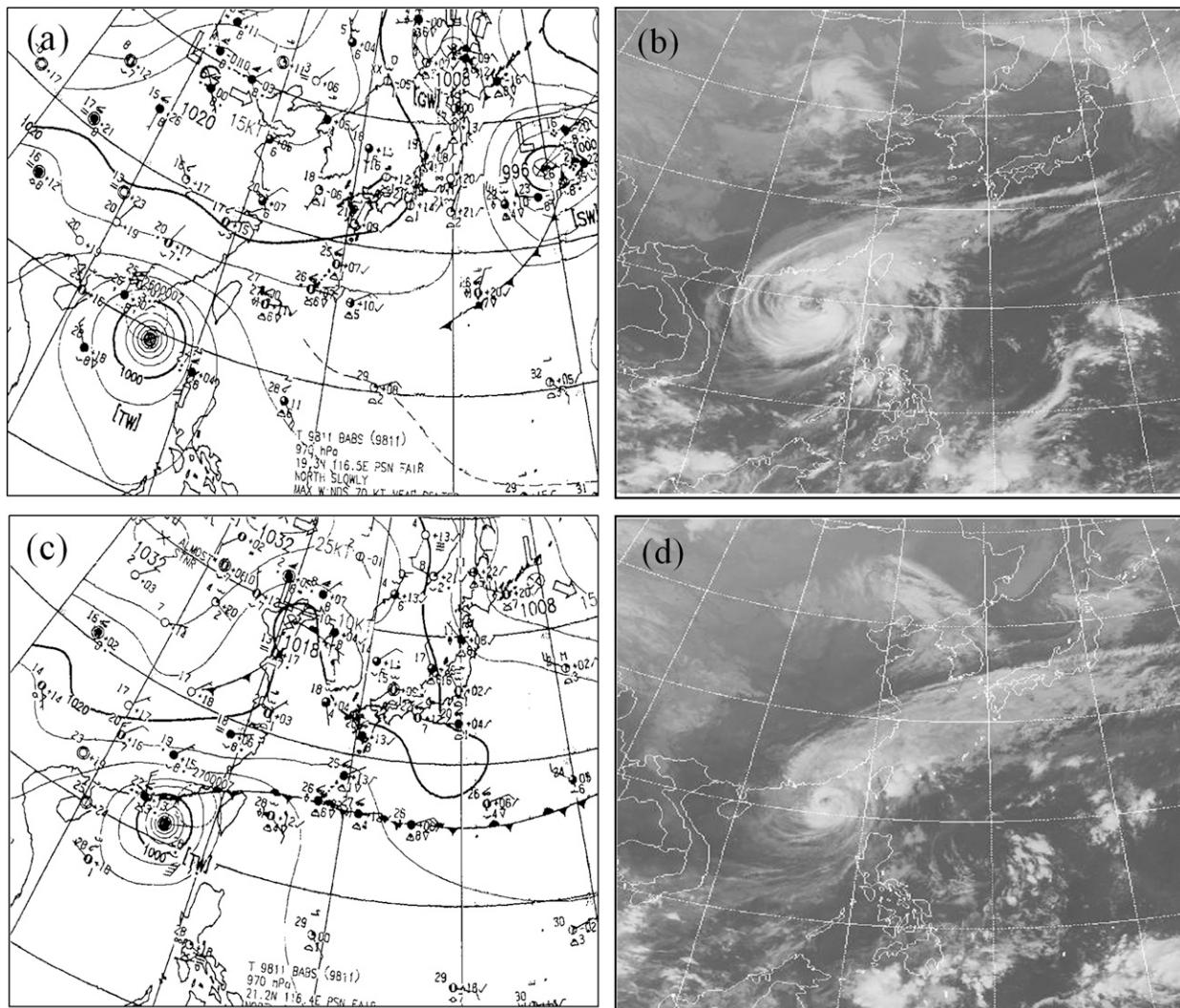
FIG. 1. (a) Surface weather map [Japan Meteorological Agency (JMA)] and (b) geostationary meteorological satellite (GMS-5) infrared satellite imagery at 0000 UTC 25 Oct 1998. (c),(d) As in (a) and (b) but at 0000 UTC 26 Oct 1998.

midlatitude cyclone and high pressure system near Japan migrated eastward rapidly and induced Babs to turn northwestward and then northward (Figs. 1a and 2a). Besides convection in the TC core region, a cloud band north of Babs's center was also found where its warm air met cold air from the north (Fig. 1b). At 0000 UTC 26 October the monsoonal cold high further intensified to generate a near-stationary frontal system just north of Taiwan (Figs. 1c,d). Typhoon Babs was steered by the prefrontal southwesterlies and turned northeastward into the Taiwan Strait. With influence from the cold monsoonal air mass that suppressed convection, Babs started to weaken and eventually dissipated over the Taiwan Strait at around 1800 UTC 27 October when its center was just off the coast of Fujian province of China.

The circulation of Typhoon Babs during 24–26 October converged with the monsoonal cold air from the north in regions east of Taiwan. These regions with strong low-level convergence were favorable for convection development and thus generated heavy rainfall. Convection was further enhanced over land by the general uplifting environment near a frontal zone and topography of Taiwan. The result of these factors was that in these three days, the accumulated rainfall in some areas of northeastern Taiwan was over 900 mm and over 700 mm on the east coast of Taiwan (Fig. 3a). Some rain stations recorded enormous amount of rain. For example, a station at Yilan (station code CIU69, near 24.63°N, 121.74°E) recorded an accumulated rainfall of 1306 mm and another one at Hualian (station code CIT95, near 23.67°N, 121.36°E) recorded 949 mm

TABLE 1. Design of the experiments performed in this study.

Name of expt	Description
E20_KF	Control run with resolution of 20 km and the Kain–Fritsch cumulus parameterization. The bogus vortex in the initial condition has a central sea level pressure of 967 hPa and a radius of 760 km.
E20_BM	As in E20_KF, but with the Betts–Miller parameterization.
E20_AK	As in E20_KF, but with the Anthes–Kuo parameterization.
E6.67_KF	As in E20_KF, but the resolution is 6.67 km.
E20_NT	No-terrain experiment: As in E20_KF, but that the terrain of Taiwan is absent in the model
E20_small	As in E20_KF, but the bogus vortex radius is 400 km.
E20_NTY	No-typhoon experiment: As in E20_KF, but no bogus vortex is added to the filtered environmental field.
E20_M1	As in E20_KF, but the 1000–700-hPa relative vorticity in monsoon region is reduced by half in the initial condition
E20_M2	As in E20_KF, but the 1000–300-hPa relative vorticity in monsoon region is reduced by half in the initial condition

of rain. This rainfall distribution that concentrated at eastern and northeastern Taiwan is actually quite typical of wintertime tropical cyclones in the vicinity of southern Taiwan, especially of those which move northward during their interaction with the monsoon circulation (Cheung et al. 2008).

3. Model setup and experimental design

The fifth-generation Pennsylvania State University–National Center for Atmospheric Research (PSU–NCAR) Mesoscale Model (MM5; Grell et al. 1995) is utilized for this study. Three domains of horizontal resolution 60, 20, and 6.67 km are used. The coarse and middle domains cover the approximate regions 3°–45°N, 100°–150°E and 10°–30°N, 110°–130°E, respectively, and they are two-way interactive during integration. Note that the finest resolution domain (center at the Taiwan area) is one-way interactive, it does not affect the results in the middle domain. Twenty-seven vertical levels with sigma coordinates are used. All the model simulations are performed from 0000 UTC 23 to 0000 UTC 26 Oct 1998.

Global analyses from the European Centre for Medium-range Weather Forecast (ECMWF) with 2.5° × 2.5° latitude–longitude resolution are used to initialize the MM5 model. However, the low resolution of the ECMWF analyses cannot resolve the structure of Typhoon Babs adequately, thus affecting its intensification in the simulations. Therefore, a spunup vortex is added to the model initial fields for better representation of Babs's structure. Following Wu et al. (2002), the spunup vortex is obtained by first performing a 12-h simulation before the initial time (i.e., starting from 1200 UTC 22 October) with a bogus vortex of radius of maximum wind 100 km and size 760 km (i.e., where vortex wind

speed becomes zero) that follows the Rankine radial profile of tangential wind (Fig. 8a). This spunup vortex maintains dynamical balance with the synoptic fields after this 12-h period and is extracted from the simulated fields. On the other hand, the original weak vortex in the ECMWF analyses is filtered using the technique as in Kurihara et al. (1995) to obtain the environmental field. The model is initialized with the spunup vortex added to the environmental field at the best-track position of Joint Typhoon Warning Center (JTWC).

The moisture physics in the model include the Kain–Fritsch in the control run (Kain and Fritsch 1993), and Betts–Miller (Betts and Miller 1986) and Anthes–Kuo (Kuo 1974; Anthes 1977) cumulus convection parameterizations in the sensitivity runs. Reisner mixed-phase microphysics (Reisner et al. 1998), radiation scheme following Dudhia (1989), and the Blackadar boundary layer parameterization are used. A total of eight numerical experiments are performed in this study (Table 1). Some of these combine different horizontal resolutions and cumulus convection schemes, and others simulate situations without terrain, with reduced TC size or modified monsoon strength, which will be discussed in detail in the following section.

4. Simulation results

a. The control experiment

The simulation with 20-km horizontal resolution and the Kain–Fritsch convection parameterization (E20_KF) is assigned as the control experiment for reference of other simulations. The simulated vortex of Babs in E20_KF moves northwestward after leaving Luzon, which is on the poleward side of the CWB best track (Fig. 2a). The position error for 12-h simulation is
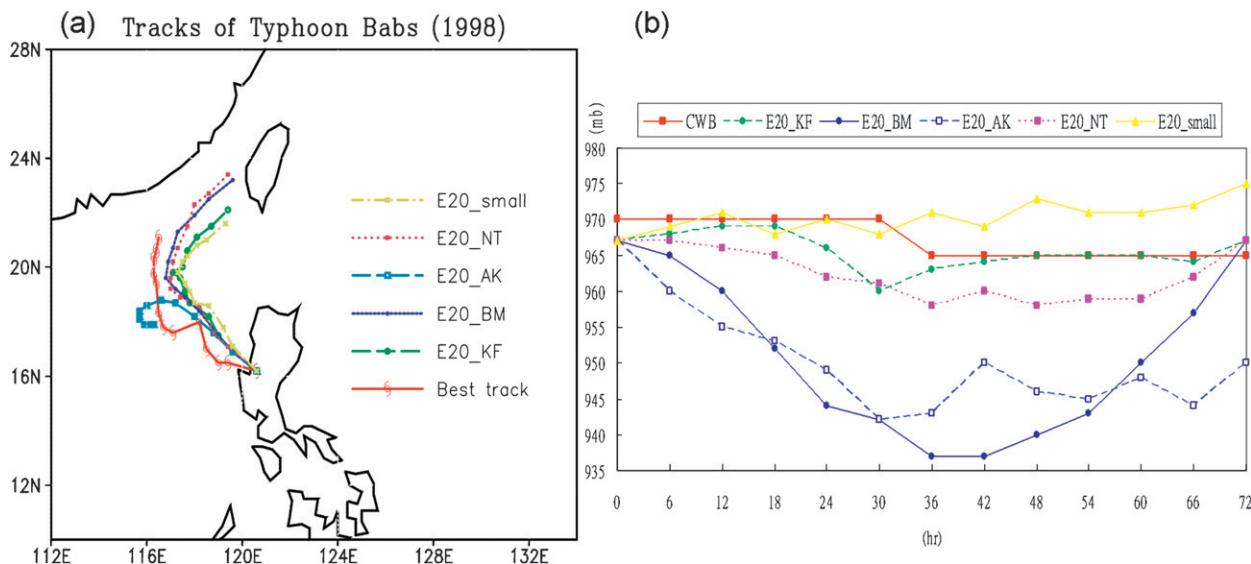
FIG. 2. (a) CWB best track and simulated tracks with six-hourly positions and (b) simulated minimum sea level pressure (hPa) of Typhoon Babs from 0000 UTC 23 to 0000 UTC 26 Oct 1998 for five of the experiments in this study.

111 km, but because of the slight northward jump of the best track position at 0000 UTC 24 October, the position error is only 89 km for 24-h simulation (Table 2). The simulated track continues northwestward for about a day, then turns northeastward and approaches Taiwan island at the end of simulation. Because of the initial directional bias and slightly higher speed in movement, the simulated 72-h position in E20_KF has an error of 301 km.

The central sea level pressure in the CWB best track for Typhoon Babs is used to validate intensity simulation because it should be more reliable than the wind-based intensity in the JTWC best track when part of Babs's circulation was under the influence of topography. Whereas the JTWC data indicates that Babs was weakening gradually from 80 kt to 70–75 kt during 0000 UTC 23 October–0000 UTC 26 October, CWB data indicates a slight drop in sea level pressure from 970 to 965 hPa at 1200 UTC 24 October (Fig. 2b). The simulated vortex in E20_KF starts with a sea level pressure of about 967 hPa, deepening in the first 30 h to about 960 hPa and then maintains at about 965 hPa. Although there was not an abrupt change in the intensity of Babs during the period of study to validate the MM5 model more rigorously, the simulated vortex intensity in this control experiment is close to that observed throughout the period, and therefore other aspects of simulation such as divergence and precipitation can be further examined.

The maximum simulated accumulated 72-h rainfall in E20_KF occurs in two areas: one at northeastern Taiwan and the other at the east coast (Fig. 3b), which is quite

similar to the observed rainfall pattern in Fig. 3a except that the amount of maximum rainfall is approximately one-third lower. Detailed examination of the sequence of rainfall during the three-day period indicates that only slight rainfall is obtained on the first day (0000 UTC 23 October–0000 UTC 24 October) because of the inflow of monsoonal northeasterlies. On the second day (0000 UTC 24 October–0000 UTC 25 October) the center of Babs is at about 20°N, 117°E, and a strong low-level convergence between northeasterlies and easterlies associated with Babs's circulation is found at northeastern Taiwan where rainfall concentrates (Fig. 4a). Rainfall in this day can be described as under the monsoon mode because interaction between the monsoon and TC circulation seems to be the dominating mechanism. Then during 0000 UTC 25 October–0000 UTC 26 October Typhoon Babs moves closer to southwest of Taiwan, and consequently strong southeasterlies impinge on the east side of CMR to cause low-level convergence (Fig. 4b). As a consequence, rainfall in this last day of simulation covers the entire east coast of Taiwan and can be

TABLE 2. Forecast track errors of five of the experiments in this study.

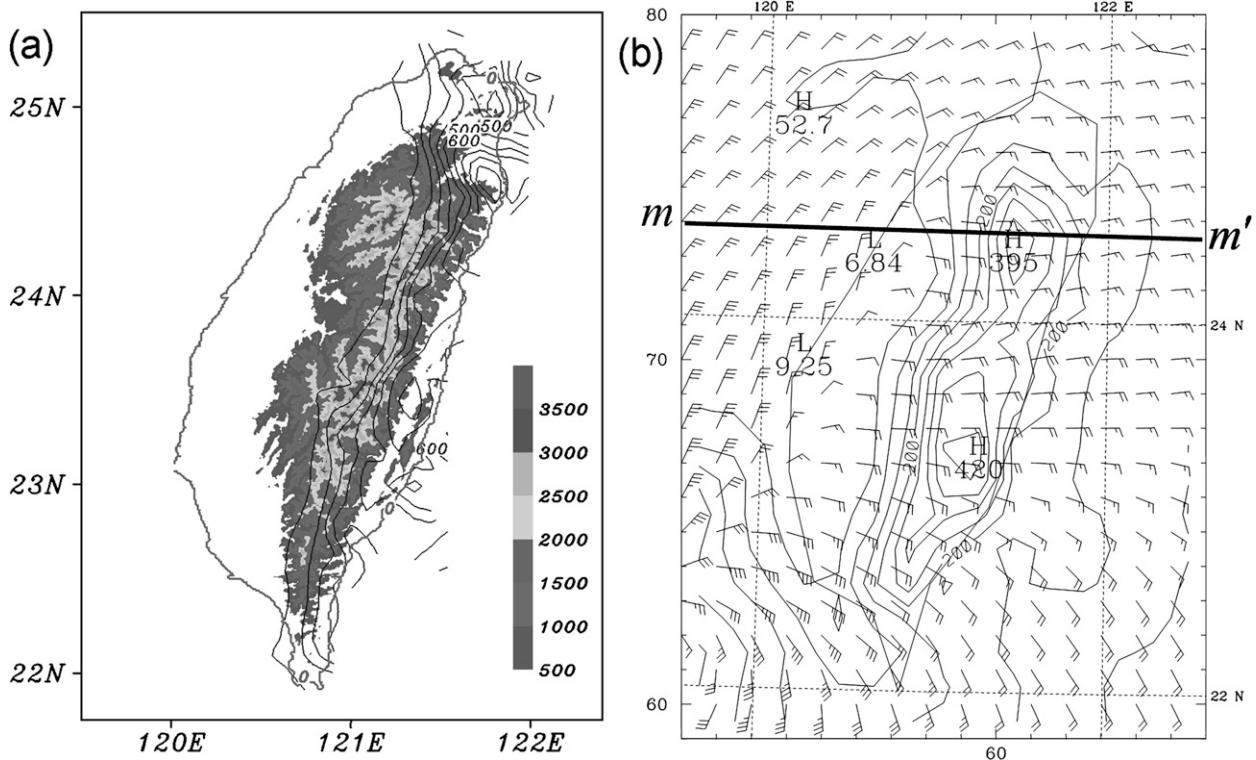| Track error (km)	0 h	12 h	24 h	36 h	48 h	60 h	72 h
E20_KF	0	111	89	213	133	198	301
E20_BM	0	110	111	156	148	216	314
E20_AK	0	146	157	200	79	133	84
E20_small	0	146	81	202	146	186	275
E20_NT	0	124	131	203	172	277	378

FIG. 3. (a) Observed and (b) simulated accumulated rainfall (contour interval of 50 mm) in experiment E20_KF from 0000 UTC 23 to 0000 UTC 26 Oct 1998. Also shown in (b) is 900-hPa simulated wind field at 0000 UTC 26 Oct (one full wind barb = 10 m s^{-1}).

described as under the topographic mode because of the blocking and uplifting effects of the CMR. It should be noted that the two rainfall modes designated here are not supposed to be exclusive to each other but that relative contributions from them seem to be affecting the rainfall budget in the region where a typhoon interacts with the winter monsoon. For example, it is believed that orographic lifting of the incoming easterlies and northeasterlies still contributes to part of the rainfall in the monsoon mode (see later discussion of the no-terrain experiment and reduction of rainfall in northeastern Taiwan). Another way to distinguish the two modes of rainfall is the change of direction of wind from northeasterlies to easterlies/southeasterlies off the coast of northeastern Taiwan. In addition, the simulated rainfall sequence described above is similar to that observed at the rain stations in Taiwan, and hence the control experiment of E20_KF should have largely captured the major synoptic mechanisms in the area.

Lin et al. (2002) discussed orographic influence on track deflection of TCs based on the basic-flow Froude number, U/Nh (U is the low-level wind speed, N is the Brunt–Väisälä frequency, and h is the terrain height), and the vortex Froude number, V_{max}/Nh (V_{max} is the TC maximum tangential wind). Whereas Typhoon Babs is

not a landfalling case and its track is less affected by Taiwan's terrain, the two Froude numbers can be used to understand the transition from the monsoonal mode of rainfall to the topographic mode. During 0000 UTC 24 October–0000 UTC 25 October, Babs's outer circulation enhances the northeasterly monsoon to increase the low-level wind speed and thus a larger basic-flow Froude number. Consequently, blocking of the flow by terrain at northeastern Taiwan is less, and major rainfall mechanism is convection forced by convergence of Babs's circulation and the northeasterly monsoon. During 0000 UTC 25 October–0000 UTC 26 October when Babs moves closer to Taiwan, the vortex Froude number at eastern Taiwan increases, and more air parcels associated with the typhoon vortex pass over the CMR, thus leading to higher orographic rainfall.

There are two other experiments, E20_BM and E20_AK that utilize the Betts–Miller and Anthes–Kuo cumulus parameterization schemes, respectively, with the same horizontal resolution. While slightly different tracks and intensification processes of Typhoon Babs are simulated in these two sensitivity experiments as compared with the control run (Fig. 2; Table 2), their simulated rainfall distributions are similar (not shown). Since the focus of this study is not on model physics
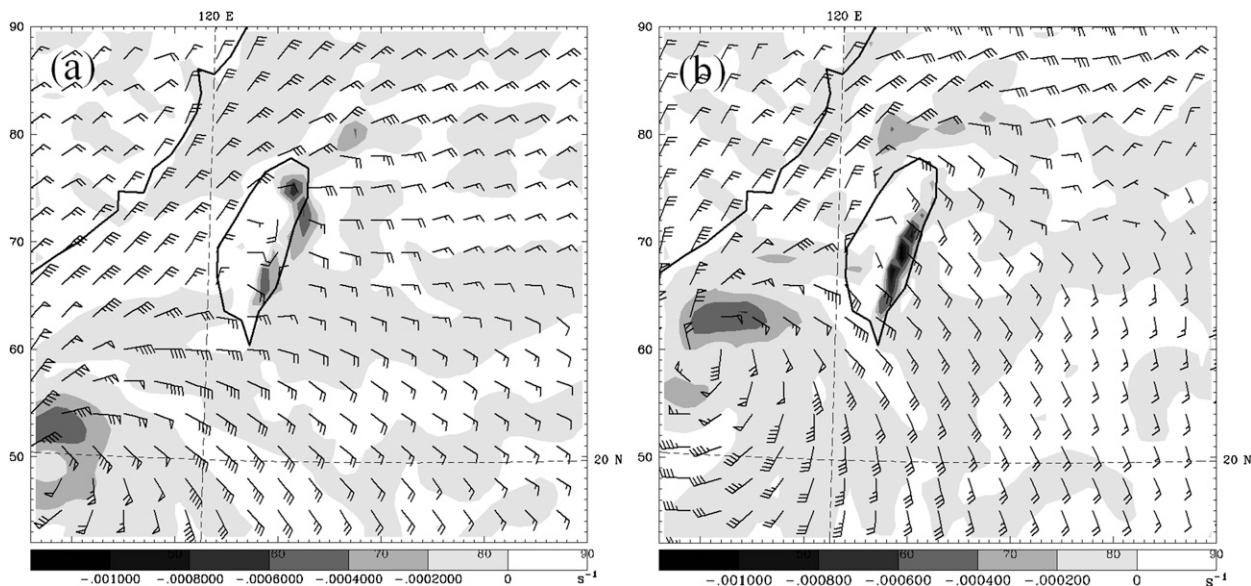
FIG. 4. Simulated 1000-hPa wind field (one full wind barb = 5 m s^{-1}) and divergence (shaded, contour interval is 2×10^{-4} s^{-1}) in experiment E20_KF at (a) 0000 UTC 25 and (b) 0000 UTC 26 Oct 1998.

intercomparison, factors leading to the different results from E20_BM and E20_AK are not further explored.

b. Sensitivity to model resolution

The simulation in the fine domain with 6.67-km horizontal resolution (E6.67_KF) reproduces a similar vortex track as in its mother domain and thus has similar position errors in all time periods (Table 2). The simulated TC vortex in this high-resolution run does not intensify much, and actually the minimum sea level pressure increases slightly during the simulation. However, the major merit of this simulation regarding rainfall forecast is that it resolves the terrain of CMR much better than the control experiment. For example, the highest altitude in the topography of E20_KF is merely 2160 m but that in E6.67_KF is 2728 m. With a better resolved CMR, the simulated topographic mode of rainfall can be more realistically captured and can consequently result in a rainfall distribution that concentrates on the windward side (Fig. 5). The maximum accumulated rainfalls of about 900 mm at two centers on the east coast are similar to the observed values, indicating that simulations with horizontal resolution below 10 km is indeed necessary for realistic rainfall forecast capability, an important issue as addressed in Wu et al. (2002).

Two more high-resolution sensitivity simulations at 6.67-km resolution that complement the no-terrain and no-typhoon experiments in the following subsections are discussed in the appendix.

c. Sensitivity to terrain

In experiment E20_NT the MM5 model configuration is the same as in E20_KF except that the topography of Taiwan is removed (i.e., altitude is set to sea level). The simulated track of Typhoon Babs in this experiment does not deviate much from that of the control experiment before its northeastward recurvature (Fig. 2a) probably because Babs's early movement was largely determined by steering from synoptic systems such as easterly trades and frontal systems, and therefore its recurvature position was over several hundred kilometers away from Taiwan. After recurvature, the simulated track in E20_NT is north of that in the control experiment and hence results in larger position errors (Table 2). The simulated vortex intensifies more than the control vortex, with a sea level pressure about 4–6 hPa lower (Fig. 2b), which may be due to removal of topography in this experiment.

The topography with steep slopes affects the precipitation by lifting moist air upslope the mountains and by modifying the heating profile from mid- to upper troposphere, which have been diagnosed in detail in Wu et al. (2002) and are not repeated here. It suffices to show that although Babs's inner-core region is not affected much by topography, uplifting of the outer-core winds are simulated in the control experiment, and moisture is retained on the upslope side of the CMR (Fig. 6a). On the contrary, moisture rapidly passes through the Taiwan area without topography in E20_NT and brings rainfall westward (Fig. 6b). The result is
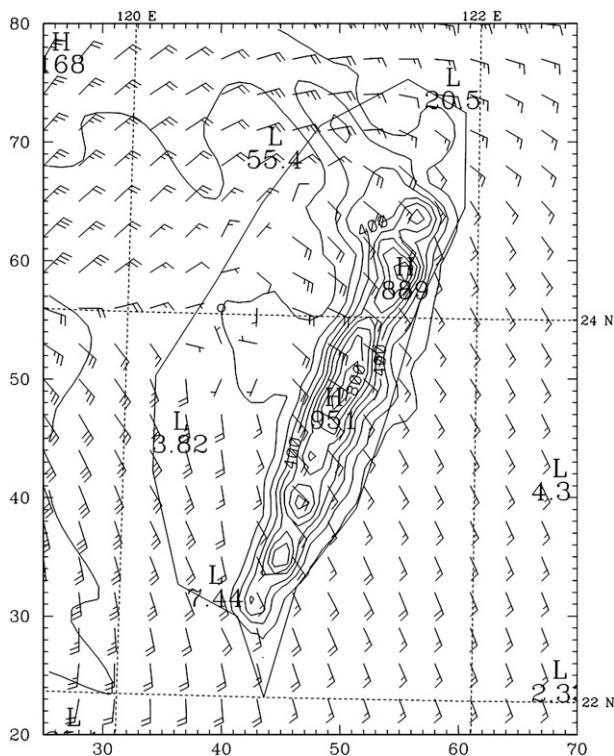
FIG. 5. As in Figs. 3b, but for experiment E6.67_KF and with contour interval of 100 mm.

that the simulated maximum accumulated rainfall in E20_NT is merely over 200 mm, which is less than half of the total rainfall in E20_KF. Rainfall concentrates at the east coast of the flattened Taiwan that may be due to enhanced convergence caused by the change in surface roughness on the east side and weaker convergence on the other side (Fig. 7a).

From the synoptic evolution point of view, the topographic mode of rainfall during 25 October is considered to be missing in the E20_NT experiment. However, it is found that interaction of Babs's circulation with the monsoonal northeasterlies is also modified by removal of topography. Low-level convergence in E20_NT at around 0000 UTC 25 October no longer concentrates at northern CMR as in the control simulation and is also lower in magnitude (Fig. 7b). This implies that the simulated heavy rainfall on this day in the control experiment is also controlled spatially by the presence of terrain and attributes in part to the uplifting effect of topography.

d. Sensitivity to the existence of a typhoon and its size

The next scenario under consideration is that the TC size, which is often not well initialized in numerical models due to lack of observations, is altered. In par-

ticular, the radius of bogus vortex is decreased from 760 km in the control simulation to 400 km in E20_small. As a consequence of this reduction, the outer-core (radius larger than 200 km) wind speed is lower than that in the original vortex for up to about 15 m s^{-1} (Fig. 8a). It is known that this change in the outer-core wind profile should not affect significantly motion of the vortex because such a change affects only the internal dynamics (Carr and Elsberry 1997). One example is the beta effect, which contributes only a small part to TC motion (Chan and Gray 1982). Indeed, as anticipated, the simulated track of Typhoon Babs in E20_small almost resembles that of the control experiment (Fig. 2a). The small vortex, however, does not intensify and its central sea level pressure actually increases slightly (Fig. 2b).

The simulated accumulated rainfall in E20_small concentrated at northern Taiwan (Fig. 8b), which is similar in magnitude to the rainfall of the same region in the control experiment, but little rainfall is obtained in the southeastern region. With weakened outer-core strength in the bogus vortex, the interaction of TC circulation with northeasterly monsoon is reduced, and so is the orographically induced rainfall at eastern Taiwan, because of its dependence on horizontal wind speed that impinges on upslope side of CMR (Chiao and Lin 2003). In terms of the two-mode picture of rainfall mechanisms during 24–26 October depicted earlier, effects from both the monsoon and topographic modes are reduced in this experiment. The fact that an appreciable amount of rainfall is received at northern Taiwan is because of the modification of the frontal system evolution north of the typhoon. In the control experiment E20_KF, the cold front starts to develop at around 0000 UTC 25 October and approaches northern Taiwan in the following day (Figs. 9a,b). Moderate 12-h accumulated rainfall of 100–200 mm is obtained at the frontal area. On the other hand, this cold front development commences as early as 0000 UTC 24 October in experiment E20_small and starts to generate rainfall in northern Taiwan (not shown). With smaller radial size in the cyclonic circulation associated with Babs, the environmental southerly wind component that originally persists east of the Philippines extends to the ocean area east of Taiwan (Figs. 9c,d). The strengthened southerly wind enables larger low-level convergence at the cold front and generated 12-h accumulated rainfall of 200–400 mm, which is much higher than that in the control simulation. Moreover, the rainfall associated with cold fronts often concentrates at the frontal zone as well as at the postfrontal zone that covers the entire northern Taiwan, which also explains why the maximum simulated rain in this experiment can extend to the west of the CMR.
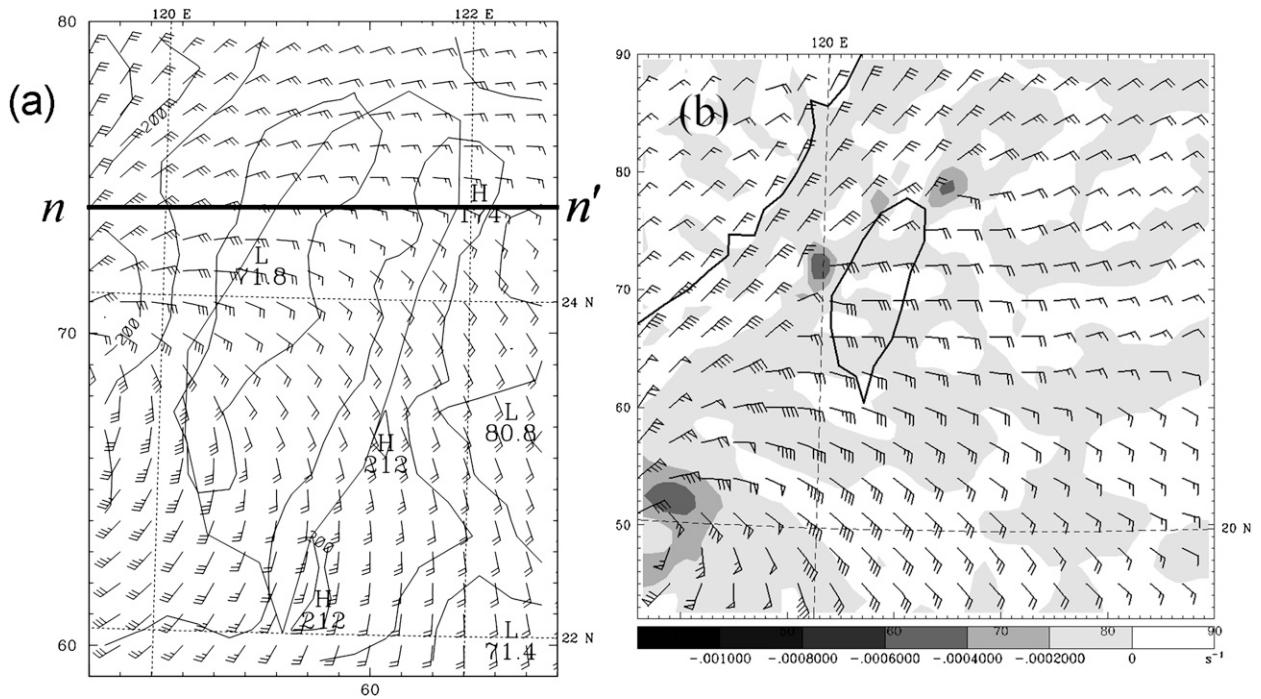
FIG. 6. (a) As in Figs. 3b, and (b) as in Fig. 4a but for experiment E20_NT.

The extreme situation is one of a pure frontal mode of rainfall when no typhoon exists, which is simulated in experiment E20_NTY without addition of a bogus vortex to the filtered environmental field. In this simu-

lation, the northeasterlies with its magnitude stronger than that in the control experiment persist in area northeast of Taiwan in the first two days (not shown). By the end of the simulation, the cold front migrates
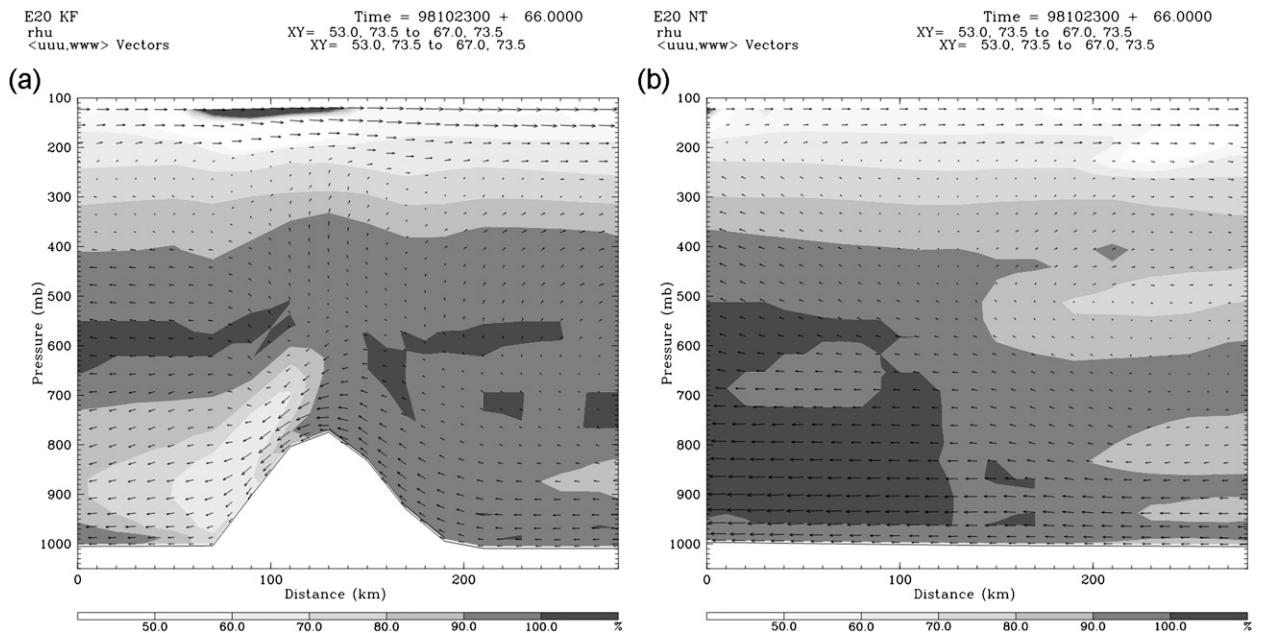
FIG. 7. East–west-oriented cross section of relative humidity (%, shaded), and zonal and vertical wind (vector) for experiment (a) E20_KF along line mm′ in Fig. 3b and (b) E20_NT along line nn′ in Fig. 7a at 1800 UTC 25 Oct 1998.
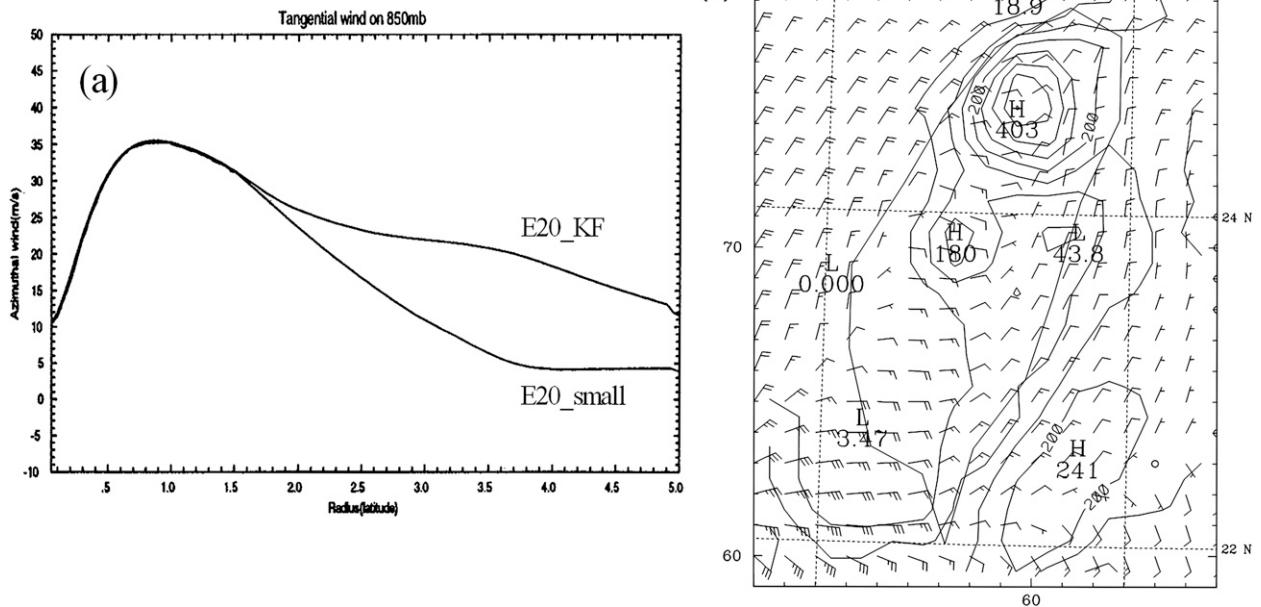
FIG. 8. (a) Azimuthally average tangential wind profiles (m s^{-1}) from center of bogus vortex in experiments E20_KF and E20_small, and (b) as in Figs. 3b, but for experiment E20_small.

southward while strong easterlies are found in the same area (Fig. 10). As anticipated, the simulated rainfall in E20_NTY is very different from previous experiments with the presence of TC circulation: combination of convection at the cold front and orographic lifting of the easterlies restricts the rainfall to northeastern Taiwan, and the total accumulated amount is about one forth less than that in E20_small.

e. Sensitivity to monsoon strength

Another possible perturbation to the typhoon–monsoon system is modification in the strength of the monsoon circulation, but with the TC circulation maintained as in the control simulation, which is performed in experiments E20_M1 and E20_M2. Unlike TC circulation with a major azimuthally symmetric wind component, monsoon circulation has no well-defined boundaries. Therefore a specific technique is developed to reduce wind surges in the Taiwan area associated with the winter monsoon, but also to maintain dynamical balance in the model initial condition. Examination of the ECMWF analyses indicates that in association with the high pressure system (anticyclonic flow) near 33°N, 123°E during the period of study there is a nearby center of minimum 850-hPa relative vorticity with a magnitude as low as -3.8×10^{-5} s^{-1}. The purpose of the technique is first to reduce the relative vorticity at each individual level between 1000–700 hPa (1000–300 hPa)

for experiment E20_M1 (E20_M2) in the model initial condition at 0000 UTC 23 October to half of the original value inside a circular domain with a radius of 600 km (Fig. 11a). Then the reduced relative vorticity inside this domain increases in linear proportion with radius back to the original value in the ECMWF analysis at the periphery of a larger circular domain with a radius of 1000 km. Then the streamfunction and, in turn, zonal and meridional wind components at the above levels are updated with the modified relative vorticity. After solving the nonlinear balance equation to obtain the new geopotential, the modified temperature is also obtained from the hydrostatic equation. After this procedure, the strength of the high pressure system is weakened and its position shifted northward in the model initial condition, and thus the magnitude of northeasterlies in South China is reduced by about half (Fig. 11b).

Responses to the reduced monsoon strength in experiments E20_M1 and E20_M2 are substantially different from each other. The simulated track of Typhoon Babs is almost the same as in the control experiment when only the low-level (1000–700 hPa) structure of monsoon circulation is modified in E20_M1. However, the simulated track in E20_M2 is biased eastward throughout the period when the deep-layer monsoon structure (1000–300 hPa) is also changed (not shown). This is consistent with previous studies that show higher
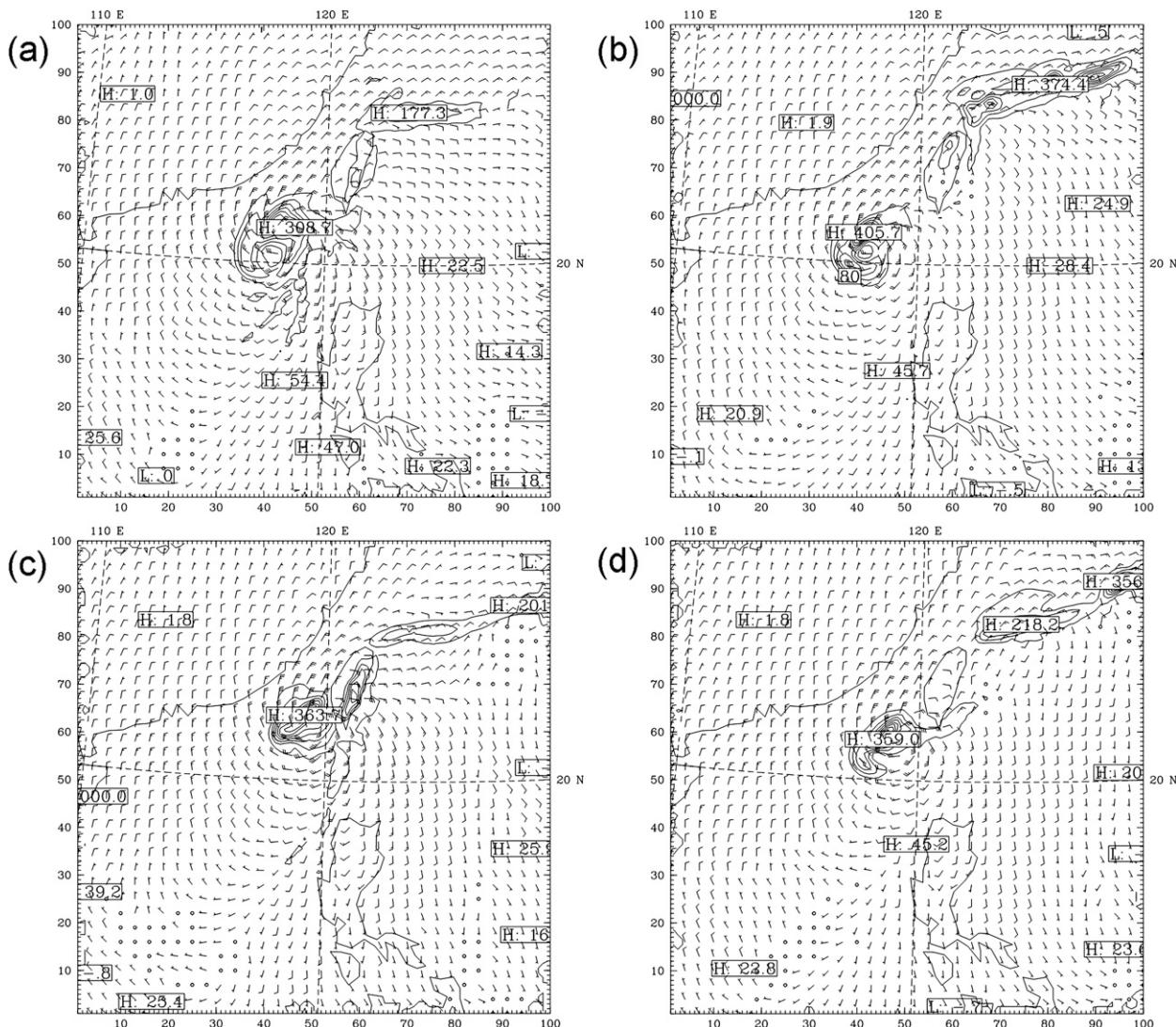
FIG. 9. Simulated 1000-hPa wind field (one full wind barb = 10 m s^{-1}) and 12-h accumulated rainfall (contour interval of 50 mm) in experiment (a) E20_KF and (b) E20_small valid at 1200 UTC 25 Oct 1998. (c),(d) As in (a),(b) but valid at 0000 UTC 26 Oct 1998.

correlation between TC motion and deep-layer steering flow than each single level (Chan and Gray 1982).

Therefore, simulated results from E20_M1 are quite comparable with the control experiment in the sense that the relative position of Typhoon Babs and Taiwan's topography is almost identical, and that differences between the two should attribute mostly to the modified low-level monsoon circulation. Indeed, locations of maximum low-level convergence between TC and monsoon circulation in eastern and northeastern Taiwan during the second day of simulation (0000 UTC 24 October–0000 UTC 25 October) in E20_M1 are similar to those in E20_KF, except that the magnitude is slightly lower (cf. Figs. 12a and 4a). The convergence in the area northeast of Taiwan seems to be lower in

E20_M1 because of the reduced wind speed in the Taiwan Strait. In the last day of simulation (0000 UTC 25 October–0000 UTC 26 October), orographic effect is mainly responsible for the rainfall at eastern Taiwan and this is also the situation in E20_M1 as the TC circulation is playing its dominating role during this day (cf. Figs. 12b and 4b). The simulated total accumulated rainfall in E20_M1 has a similar distribution as in the control experiment; that is, a maximum in northeast Taiwan and another in eastern Taiwan, but with the maximum values about one-fourth lower because of the reduced rainfall in the monsoon mode.

Because the simulated typhoon center in E20_M2 is closer to the Taiwan island and eventually makes landfall near the end of simulation, strong low-level
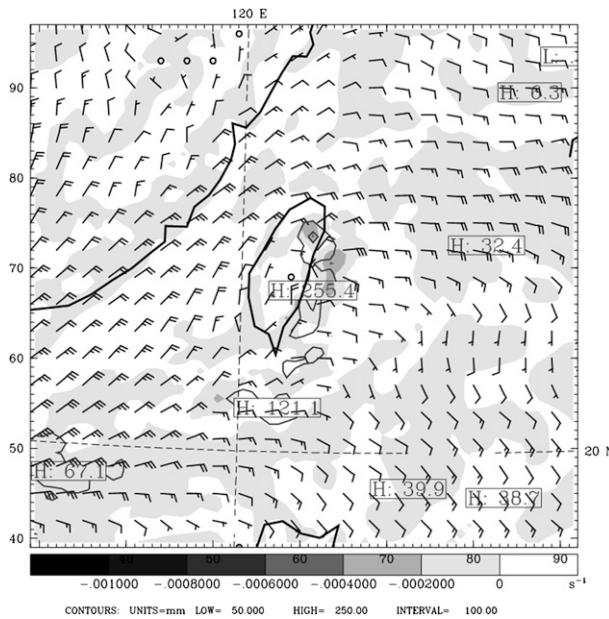
FIG. 10. As in Fig. 4b, but for experiment E20_NTY.

convergence and hence convection are found over eastern Taiwan because of the orographic lifting throughout the period of 24–26 October (Figs. 12c,d). As a consequence, simulated total accumulated rainfall in E20_M2 is similar in magnitude to that in the control experiment but with entirely different contributions from the various modes of rainfall. Because of the simulated TC

track change due to modification in the monsoon deep-layer circulation, rainfall in the Taiwan area can be said to undergo a transition to the topographic mode throughout the period of study. The northeastward-biased TC position during the last day of simulation in E20_M2 also modifies evolution of the frontal system to the north, and thus results in a different rainfall budget in the large Southeast Asia area.

5. Summary and discussion

In summary, the heavy rainfall event in the Taiwan area associated with interaction between Typhoon Babs (1998) and the East Asia winter monsoon is studied. After its formation in the western North Pacific in mid-October, Babs first moved westward while intensifying to supertyphoon before making landfall to the Philippines, but it started weakening while entering the South China Sea. At around 0000 UTC 25 October, Babs turned northward and then northeastward because of influences from the monsoon circulation and eastward migration of a cold front. Eventually the typhoon dissipated over the Taiwan Strait at about 1800 UTC 27 October without a second landfall.

During the period when Babs was in the South China Sea, the interaction among the typhoon, northeasterly monsoon, and cold frontal system induced heavy rainfall in Taiwan, which was further enhanced by topographic effects. The accumulated rainfall during 0000 UTC
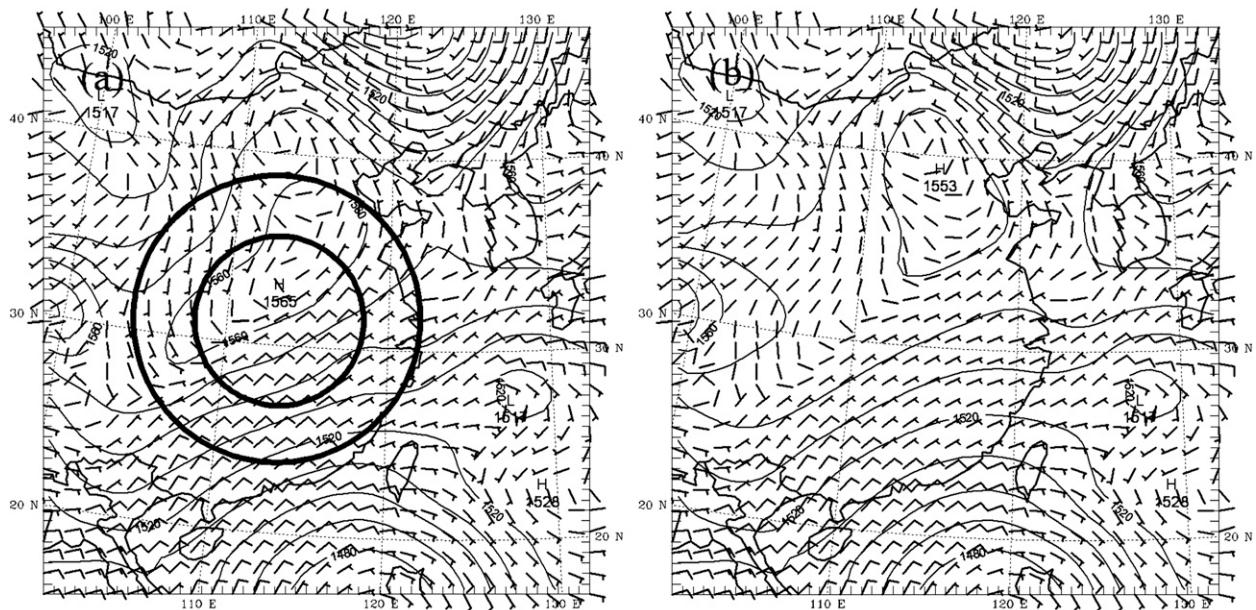

FIG. 11. The 850-hPa geopotential height (contour, m) and wind field (one full wind barb = 10 m s^{-1}) in coarse domain of (a) model initial condition for control experiment E20_KF, and (b) modified model initial condition for experiment E20_M1 at the same level with reduced relative vorticity in circular regions in (a), see section 4e for details of technique used.
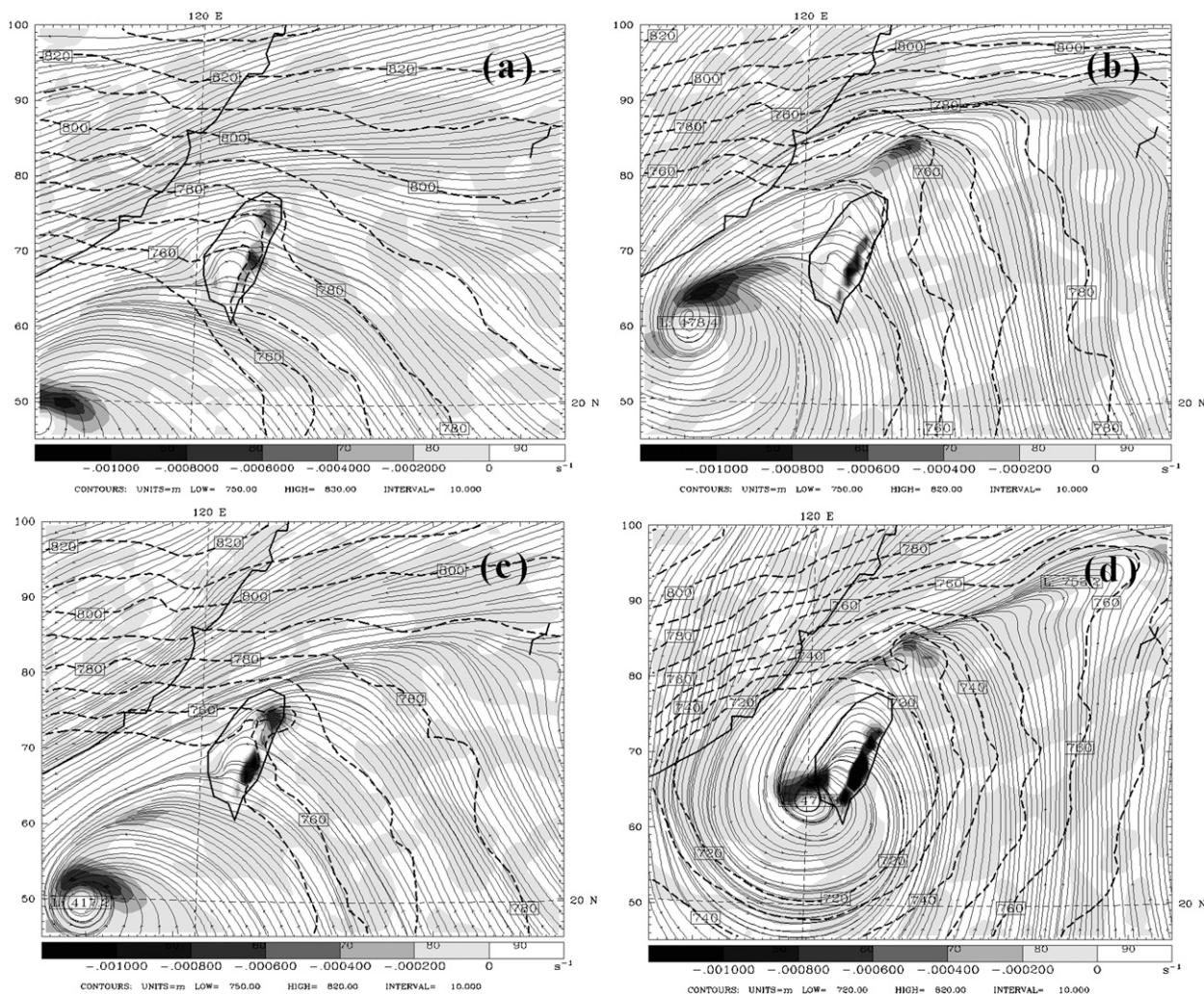
FIG. 12. Simulated 925-hPa streamline, geopotential height (dashed line, m) and divergence (shaded, contour interval is 2×10^{-4} s^{-1}) in experiment E20_M1 at (a) 1800 UTC 24 and (b) 0000 UTC 26 Oct. (c),(d) As in (a),(b) but for experiment E20_M2.

23 October–0000 UTC 26 October in some areas in northeastern Taiwan exceeded 900 mm, and the rainfall at some other areas on the east coast exceeded 700 mm. This heavy rainfall event is simulated in this study using the MM5 with three nested domains and a highest horizontal resolution of 6.67 km. A series of sensitivity experiments that include model physics, terrain effect, typhoon vortex structure, and monsoon strength is performed, aiming at investigating the predictability of this typhoon–monsoon–terrain system when some of its components are perturbed. The experiments with different cumulus parameterization schemes show that the simulations with Kain–Fritsch parameterization (E20_KF and E6.67_KF) are the best in terms of capturing both simulated track and intensity. The 20-km resolution simulation reproduces the correct rainfall distribution during the three days under study, and the fine domain

with 6.67-km resolution further improves the maximum simulated rainfall to very close to observations. Therefore simulation E20_KF is considered the control experiment in this study on which the comparison for other sensitivity experiments with 20-km resolution is based.

The rainfall event is diagnosed as consisting of two major modes of occurrence, as shown in the schematic diagram (Fig. 13) of the rainfall mechanisms associated with the monsoon mode and the topographic mode, as a response to the interaction among the typhoon circulation, northeasterly monsoon flow, and terrain of Taiwan. During 0000 UTC 24 October–0000 UTC 25 October, rainfall that concentrates in northeastern Taiwan is mostly the result of the low-level convergence between the typhoon circulation and monsoonal northeasterlies, and this is described as the monsoon mode. On the next
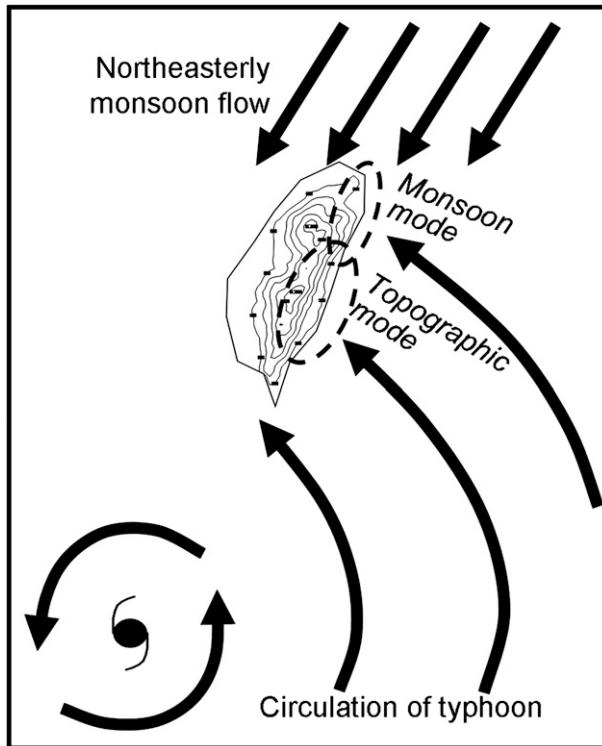
FIG. 13. Schematic diagram of the rainfall mechanisms associated with the monsoon mode and the topographic mode, as a response to the interaction among the typhoon circulation, northeasterly monsoon flow, and terrain of Taiwan (contour interval of 500 m).

day, during 0000 UTC 25 October–0000 UTC 26 October, impingement of typhoon circulation on the CMR of Taiwan becomes the major mechanism of rainfall that concentrate on the east coast, and therefore this process is designated as the topographic mode. As anticipated, removal of the Taiwan terrain in one of the sensitivity experiments (E20_NT) results in completely different rainfall distribution due to the lack of convection by orographic lifting. However, this is not the only role played by terrain in regard to rainfall generation in that the low-level convergence pattern between the typhoon circulation and monsoonal northeasterlies changes as well in the simulation without terrain. It is therefore believed that the terrain, with its specific orientation with respect to the typhoon, also plays a role of modulating the monsoonal flow and typhoon circulation such that the position of strong convergence between the two systems and thus the subsequent location with the maximum rainfall is variable.

There are two sensitivity experiments in which Typhoon Babs's size is changed: In E20_small the radius of the bogus vortex is reduced, and in the extreme case of E20_NTY no bogus vortex is added at all, and MM5's

model initial condition remains the filtered environmental field. Simulation results in these two experiments reveal reduced interaction in both the monsoon and topography modes when wind speed in the outer-core region of the typhoon gets weaker. Because there is no typhoon vortex to interact with monsoon circulation in E20_NTY, rainfall is mainly associated with evolution of the cold frontal system (pure frontal mode). Notably, when the typhoon size is altered, evolution of the cold front is modified substantially. In the case of E20_small, the frontal position migrates southward in a faster pace than the control simulation, and the rain rate at the front also increased such that total accumulated rainfall at northern Taiwan is comparable with that in the control simulation, but with shifted maximum position. Consequently, rainfall is not restricted on the eastern side of the central mountain range but may extend to the entire northern region.

The last component to perturb in the system interaction picture of the heavy rainfall event is the monsoon system. A technique is developed to modify the monsoon strength in the South China region, so that the dynamical balance is maintained in the model initial condition. The method is to start from a regional change in relative vorticity and then perform successive update of the streamfunction, wind field, geopotential, and temperature by solving the nonlinear balance and hydrostatic equations. Simulation results in experiment E20_M1 indicate that low-level (1000–700 hPa) reduction in monsoon strength weakens interaction with the typhoon, but rain distribution remains the same as in the control simulation. However, it is found in experiment E20_M2 that the simulated typhoon track is quite sensitive to the deep layer (1000–300 hPa) monsoon strength. When the typhoon moves closer to the island of Taiwan in this experiment, topographic effect to rainfall enhances substantially. Although the simulated rainfall amount is close to observation, the underlying mechanisms are incorrect.

The direct question to be asked after this system analysis of Typhoon Babs is, how representative this rainfall pattern is and how often does this type of interaction occur? If the TC best track database in the Taiwan area is examined, and all historical TCs entering the area are classified roughly as either westward moving or northward moving, the ratio of the number of TCs in the two classes is approximately 3/2. That is, those TCs that recurve at lower latitudes and move northward, and those that originate in the SCS and move northward account for about 40% of all cases in the area. Among these 40% cases, those that occur during the winter monsoon have an opportunity to confront strong northeasterlies and cold fronts just as in the

case of Typhoon Babs. Therefore, Typhoons Babs and Lynn mentioned in the introduction are just extreme examples in which exceptionally high rainfall occurred, but this kind of typhoon–monsoon–terrain interaction to different degrees should not be very rare.

The point to note here is that the rainfall pattern associated with Typhoon Babs is not regarded as a definite map for reference to other similar cases, because obviously if the TC center is located on the different side of terrain, then rainfall distribution will be substantially altered. The conceptual model of rainfall sequence that is derived from analysis of Typhoon Babs should be established on various responses to system perturbations ever examined in the study, and that different rainfall mechanisms are playing their roles in these responses. Then this conceptual model can be applied in assessment of numerical products for real-time forecast situations. For example, if a numerical model is initialized with a simple TC vortex bogus technique without sophisticated adjustment by observations, then the likely evolution of TC structure in the simulation will not be very accurate, and estimate of the degree of TC–monsoon interaction is not highly reliable. On the other hand, if the numerical model is known as problematic in synoptic development and error in the TC track forecast is possibly large, then different scenarios of overesti-

mation and underestimation of the topographic mode of rainfall should be made given different TC–terrain distances.

APPENDIX

High-Resolution Sensitivity Experiments

Whereas most of the results in this study, in particular the processes that lead to the several modes of rainfall, are derived from the 20-km resolution MM5 simulations, concerns exist on whether the major conclusions are robust and independent of model resolution. Therefore, a third domain with 6.67-km resolution is added to experiments E20_NT and E20_NTY to become the equivalence of the control run E6.67_KF.

It is found that the situation in E6.67_NT is similar to the 20-km resolution simulation. Without Taiwan's terrain topographic rainfall does not occur and hence accumulated rainfall in the Taiwan region is minimal, while some rainbands move into the South China Sea
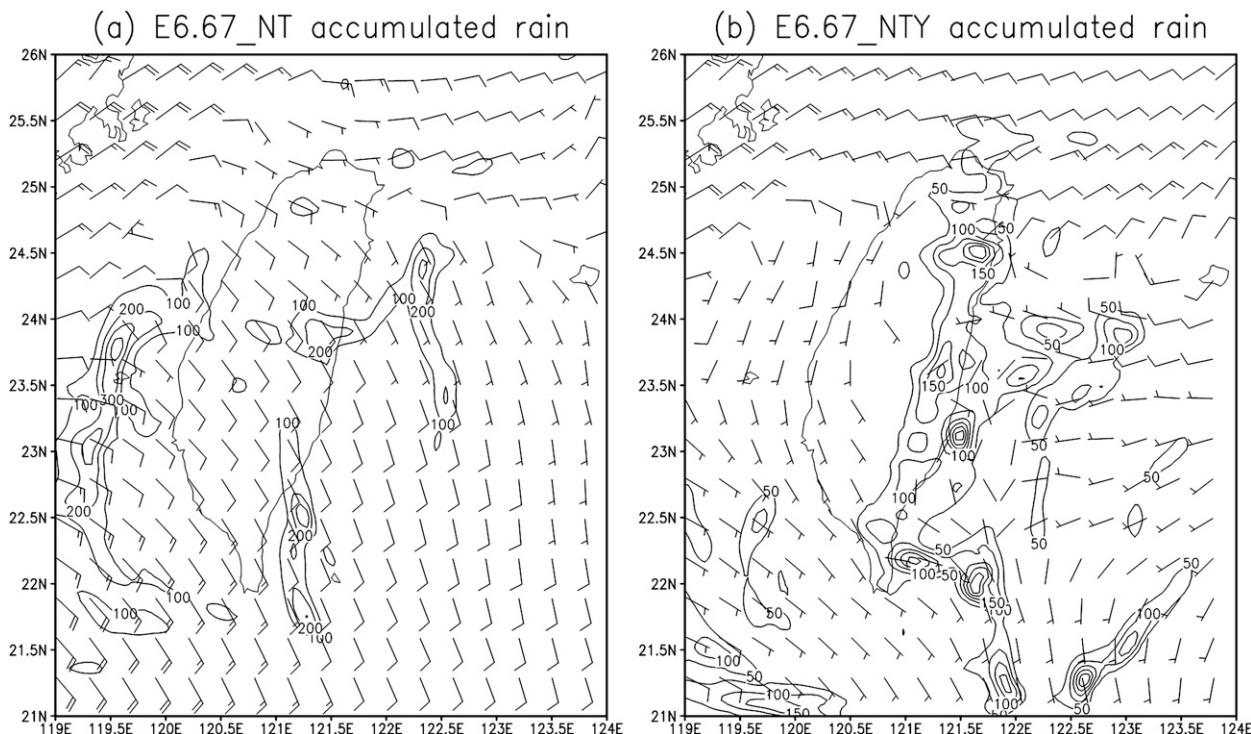

FIG. A1. As in Fig. 3b, but for the (a) no-terrain (NT) and (b) no-typhoon (NTY) simulations with 6.67-km resolution.

following the easterlies and northeasterlies (Fig. A1a). As in E20_NTY, the high-resolution simulation without Typhoon Babs's circulation also indicates that rainfall is concentrated over northeastern Taiwan because of the northeasterly monsoon. Because of the better-resolved topography in the high-resolution run, rainfall distribution does extend to the CMR area (Fig. A1b). However, the maximum accumulated rainfall of about 300 mm in this experiment is much less than the control run with the same resolution, again confirming the contrast in rainfall between the frontal mode and the combination of monsoon mode and topographic mode when Typhoon Babs plays its role.

REFERENCES

Anthes, R. A., 1977: A cumulus parameterization scheme utilizing a one-dimensional cloud model. *Mon. Wea. Rev.,* **105,** 270–286.

ATCR, 1987: *Annual Tropical Cyclone Report.* Joint Typhoon Warning Center, 218 pp.

——, 1998: *Annual Tropical Cyclone Report.* Joint Typhoon Warning Center, 211 pp.

Bender, M. A., R. E. Tuleya, and Y. Kurihara, 1987: A numerical study of the effect of island terrain on tropical cyclones. *Mon. Wea. Rev.,* **115,** 130–155.

Betts, A. K., and M. J. Miller, 1986: A new convective adjustment scheme. Part II: Single column tests using GATE wave, BOMEX, ATEX, and Arctic air-mass data sets. *Quart. J. Roy. Meteor. Soc.,* **112,** 693–709.

Brand, S., and J. W. Blelloch, 1974: Changes in the characteristics of typhoons crossing the island of Taiwan. *Mon. Wea. Rev.,* **102,** 708–713.

Carr, L. E., III, and R. L. Elsberry, 1997: Models of tropical cyclone wind distribution and beta-effect propagation for application to tropical cyclone track forecasting. *Mon. Wea. Rev.,* **125,** 3190–3209.

Chan, J. C. L., and W. M. Gray, 1982: Tropical cyclone movement and surrounding flow relationships. *Mon. Wea. Rev.,* **110,** 1354–1374.

Chang, C. P., T.-C. Yeh, and J.-M. Chen, 1993: Effects of terrain on the surface structure of typhoons over Taiwan. *Mon. Wea. Rev.,* **121,** 734–752.

Chang, S.-W., 1982: The orographic effects induced by an island mountain range on propagating tropical cyclones. *Mon. Wea. Rev.,* **110,** 1255–1270.

Cheung, K. K. W., L.-R. Huang, and C.-S. Lee, 2008: Characteristics of rainfall during tropical cyclone periods in Taiwan. *Nat. Hazards Earth Syst. Sci.,* **8,** 1463–1474.

Chien, F.-C., Y.-C. Liu, and C.-S. Lee, 2008: Heavy rainfall and southwesterly flow after the leaving of Typhoon Mindulle (2004) from Taiwan. *J. Meteor. Soc. Japan,* **86,** 17–41.

Chiao, S., and Y.-L. Lin, 2003: Numerical modeling of an orographically enhanced precipitation event associated with Tropical Storm Rachel over Taiwan. *Wea. Forecasting,* **18,** 325–344.

Dudhia, J., 1989: Numerical study of convection observed during the Winter Monsoon Experiment using a mesoscale two-dimensional model. *J. Atmos. Sci.,* **46,** 3077–3107.

Grell, G. A., J. Dudhia, and D. R. Stauffer, 1995: A description of the fifth-generation Penn State/NCAR mesoscale model (MM5). NCAR Tech. Note, NCAR/TN-398+STR, 138 pp.

Jian, G.-J., and C.-C. Wu, 2008: A numerical study of the track deflection of super-Typhoon Haitang (2005) prior to its landfall in Taiwan. *Mon. Wea. Rev.,* **136,** 598–615.

Kain, J. S., and J. M. Fritsch, 1993: Convective parameterization for mesoscale models: The Kain–Fritsch scheme. *The Representation of Cumulus Convection in Numerical Models, Meteor. Monogr.,* No. 46, Amer. Meteor., Soc., 165–170.

Kurihara, Y., M. A. Bender, R. E. Tuleya, and R. J. Ross, 1995: Improvements in the GFDL hurricane prediction system. *Mon. Wea. Rev.,* **123,** 2791–2801.

Kuo, H.-L., 1974: Further studies of the influence of cumulus convection on large-scale flow. *J. Atmos. Sci.,* **31,** 1232–1240.

Lee, C.-S., Y.-C. Liu, and F.-C. Chien, 2008: The secondary low and heavy rainfall associated with Typhoon Mindulle (2004). *Mon. Wea. Rev.,* **136,** 1260–1283.

Lin, Y.-L., D. B. Ensley, and S. Chiao, 2002: Orographic influences on rainfall and track deflection associated with the passage of a tropical cyclone. *Mon. Wea. Rev.,* **130,** 2929–2950.

——, S.-Y. Chen, C. M. Hill, and C.-Y. Huang, 2005: Control parameters for the influence of a mesoscale mountain range on cyclone track continuity and deflection. *J. Atmos. Sci.,* **62,** 1849–1866.

Lonfat, M., Jr., F. D. Marks, and S. S. Chen, 2004: Precipitation distribution in tropical cyclones using the Tropical Rainfall Measuring Mission (TRMM) microwave imager: A global perspective. *Mon. Wea. Rev.,* **132,** 1645–1660.

Reisner, J. R., M. Rasmussen, and R. T. Bruintjes, 1998: Explicit forecasting of supercooled liquid water in winter storms using the MM5 mesoscale model. *Quart. J. Roy. Meteor. Soc.,* **124,** 1071–1107.

Wu, C.-C., 2001: Numerical simulation of Typhoon Gladys (1994) and its interaction with Taiwan terrain using the GFDL hurricane model. *Mon. Wea. Rev.,* **129,** 1533–1549.

——, and Y.-H. Kuo, 1999: Typhoons affecting Taiwan—Current understanding and future challenges. *Bull. Amer. Meteor. Soc.,* **80,** 67–80.

——, T.-H. Yen, Y.-H. Kuo, and W. Wang, 2002: Rainfall simulation associated with Typhoon Herb (1996) near Taiwan. Part I: The topographic effect. *Wea. Forecasting,* **17,** 1001–1015.

Yeh, T.-C., and R. L. Elsberry, 1993a: Interaction of typhoons with the Taiwan orography. Part I: Upstream track deflection. *Mon. Wea. Rev.,* **121,** 3193–3212.

——, and ——, 1993b: Interaction of typhoons with the Taiwan orography. Part II: Continuous and discontinuous tracks across the island. *Mon. Wea. Rev.,* **121,** 3213–3233.